# k=0Magnetic Structure and Absence of Ferroelectricity in SmFeO3

KUO, C-Y., DREES, Y., FERNÁNDEZ-DÍAZ, M.T., ZHAO, L., VASYLECHKO, L., SHEPTYAKOV, D., BELL, Anthony, PI, T.W., LIN, H-J., WU, M-K., PELLEGRIN, E., VALVIDARES, S.M., LI, Z.W., ADLER, P., TODOROVA, A., KÜCHLER, R., STEPPKE, A., TJENG, L.H., HU, Z. and KOMAREK, A.C.



**Published version**

KUO, C-Y., DREES, Y., FERNÁNDEZ-DÍAZ, M.T., ZHAO, L., VASYLECHKO, L., SHEPTYAKOV, D., BELL, Anthony, PI, T.W., LIN, H-J., WU, M-K., PELLEGRIN, E., VALVIDARES, S.M., LI, Z.W., ADLER, P., TODOROVA, A., KÜCHLER, R., STEPPKE, A., TJENG, L.H., HU, Z. and KOMAREK, A.C. (2014). k=0Magnetic Structure and Absence of Ferroelectricity in SmFeO3. Physical Review Letters, 113 (21).

# $k = 0$ Magnetic Structure and Absence of Ferroelectricity in $SmFeO_3$

C.-Y. Kuo,[1] Y. Drees,[1] M. T. Fernández-Díaz,[2] L. Zhao,[3] L. Vasylechko,[1,4] D. Sheptyakov,[5] A. M. T. Bell,[6] T. W. Pi,[7] H.-J. Lin,[7] M.-K. Wu,[3] E. Pellegrin,[8] S. M. Valvidares,[8] Z. W. Li,[1] P. Adler,[1] A. Todorova,[1] R. Küchler,[1] A. Steppke,[1] L. H. Tjeng,[1] Z. Hu,[1] and A. C. Komarek[1,*]

[1]*Max-Planck-Institute for Chemical Physics of Solids, Nöthnitzer Strasse 40, 01187 Dresden, Germany*
[2]*Institut Laue-Langevin, 38042 Grenoble, France*
[3]*Institute of Physics, Academia Sinica, Taipei 11529, Taiwan*
[4]*Lviv Polytechnic National University, 12 Bandera Street, 79013 Lviv, Ukraine*
[5]*Laboratory for Neutron Scattering and Imaging, Paul Scherrer Institut, CH-5232 Villigen PSI, Switzerland*
[6]*HASYLAB at DESY, Notkestrasse 85, 22607 Hamburg, Germany*
[7]*National Synchrotron Radiation Research Center (NSRRC), 101 Hsin-Ann Road, Hsinchu 30077, Taiwan*
[8]*CELLS-ALBA Synchrotron Radiation Facility, Carretera BP 1413, km 3.3, E-08290 Cerdanyola del Vallès, Barcelona, Spain*

(Received 18 June 2014; published 20 November 2014)

$SmFeO_3$ has attracted considerable attention very recently due to its reported multiferroic properties above room temperature. We have performed powder and single crystal neutron diffraction as well as complementary polarization dependent soft X-ray absorption spectroscopy measurements on floating-zone grown $SmFeO_3$ single crystals in order to determine its magnetic structure. We found a $k = 0$ *G*-type collinear antiferromagnetic structure that is not compatible with inverse Dzyaloshinskii-Moriya interaction driven ferroelectricity. While the structural data reveal a clear sign for magneto-elastic coupling at the Néel-temperature of ~675 K, the dielectric measurements remain silent as far as ferroelectricity is concerned.

DOI: 10.1103/PhysRevLett.113.217203 PACS numbers: 75.25.-j, 61.05.fg, 75.85.+t, 77.22.-d

The discovery of magnetism induced ferroelectricity has renewed interest in multiferroic materials due to the enhanced magnetoelectric interaction in these materials that makes them very interesting for technical applications [1,2]. Recently, it has been found that ferroelectricity can arise from some special types of magnetic structures inducing sizeable magnetoelectric effects and the ability to switch the electric polarization by an applied magnetic field (and vice versa). In these recently studied materials, magnetic frustration induces a complex magnetic structure with cycloids or spirals [1]. However, also the ordering temperatures need to be above room temperature in order to make these materials interesting for technical applications. Very recently, the discovery of ferroelectric polarization in $SmFeO_3$ has been reported below $T_N \sim 670$ K. The origin of this ferroelectric polarization is highly debated [3–5]. A further spin-reorientation transition occurs at $T_{SR} \sim 480$ K in this material without having any noticeable effect on the ferroelectric polarization. In the initial publication an inverse Dzyaloshinskii-Moriya interaction based mechanism has been reported to be the driving force of the ferroelectric properties of $SmFeO_3$ [3]. The underlying $k = 0$ magnetic structure was not directly measured but calculated by *ab initio* calculations [3]. However, it has been demonstrated that this calculated $k = 0$ magnetic structure with magnetic ions located at inversion centers cannot be responsible for a spin-orbit-coupling driven ferroelectric polarization by $\mathbf{S}_i \times \mathbf{S}_j$ in this material since inversion symmetry will not be broken [4]. Within this context, an alternative mechanism based on $J\mathbf{S}_i \bullet \mathbf{S}_j$ exchange-striction has been proposed to be responsible for the ferroelectric polarization in $SmFeO_3$ [5].

Here, we report the experimentally observed magnetic structure of $SmFeO_3$ and reanalyze the ferroelectric properties of $SmFeO_3$. A large reddish $SmFeO_3$ single crystal with $T_N \sim 675$ K has been grown at a Crystal Systems Corp. 4-mirror optical floating zone furnace. The high sample quality of this insulating reddish orange single crystal has been confirmed by EDX, Laue, and x-ray diffraction techniques as well as by magnetization and Mössbauer spectroscopy measurements; see the Supplemental Materials [6]. In the inset of Fig. 1(a) a polarization microscope image is shown that indicates—together with our Laue diffraction analysis—that our $SmFeO_3$ crystals are single domain single crystals. No impurity phases are visible in highly accurate synchrotron radiation powder x-ray diffraction measurements that have been performed at beamline B2 of DORIS-III at DESY. The lattice parameters, unit cell volume and relative expansion of the lattice parameters of $SmFeO_3$ (*Pbnm* setting with $a < b < c$) are shown in Figs. 1(a), 1(b). The *b*-lattice parameter exhibits a small anomalous kink around $T_N$ that is indicative for magnetoelastic coupling at the magnetic ordering temperature $T_N$. The other lattice parameters exhibit much less pronounced anomalies at $T_N$ that are even only barely visible in the derivatives of the lattice parameters; see Figs. 1(c), 1(d).

The highly neutron absorbing properties of the element Sm (~5900 barn for 2200 m/s neutrons) hampered the

 

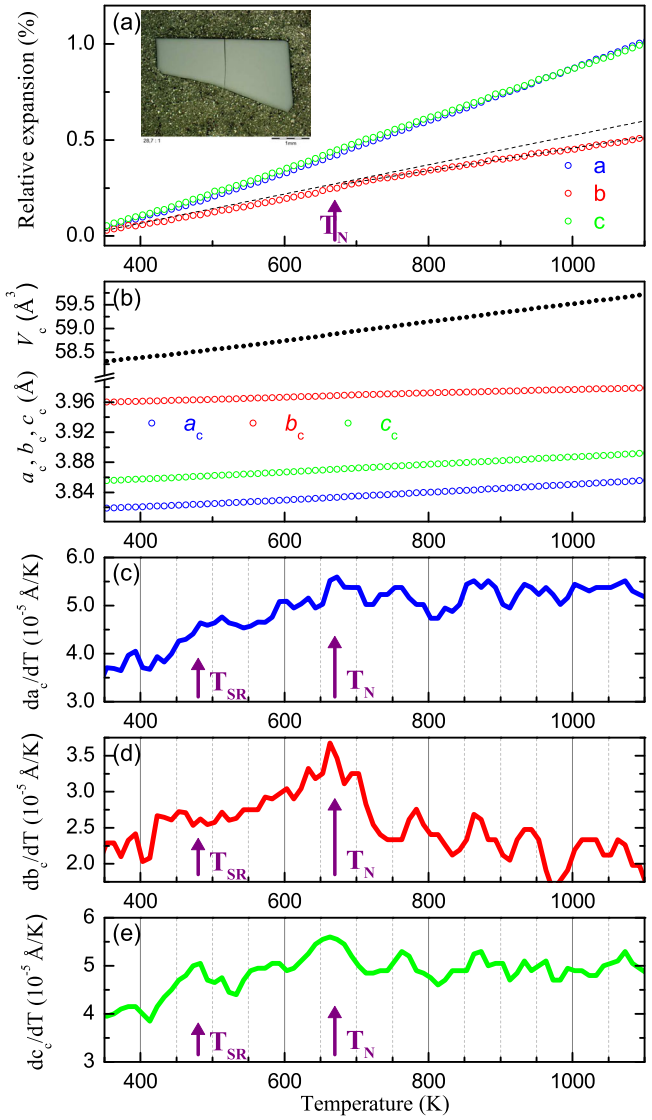


FIG. 1 (color online). Results of our synchrotron radiation powder x-ray diffraction measurements of $SmFeO_3$ obtained at beam line B2 of DORIS-III at DESY ($\lambda = 0.538163$ Å, space group $Pbnm$). (a) Relative expansion $r(a) = [a(\mathrm{T}) - a(300\ \mathrm{K})]/a(300\ \mathrm{K})$. In the inset a polarization microscope image of a single crystalline sample is shown. (b) Unit cell volume and pseudocubic lattice parameters $V_c = V/4$, $a_c = a/\sqrt{2}$, $b_c = b/\sqrt{2}$, $c_c = c/2$. (c)–(e) The derivative $da_c/dT$ of the pseudocubic lattice parameters (averaged over 4 data points). All dashed lines are guide to the eyes.

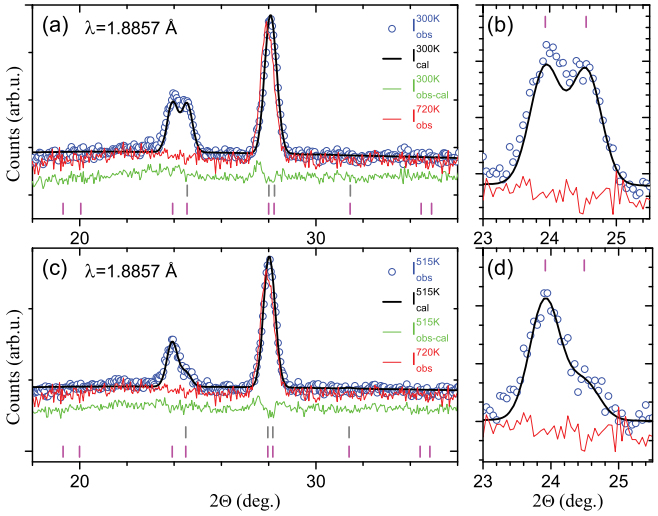


FIG. 2 (color online). Powder neutron diffraction measurements of $SmFeO_3$ at (a),(b) 300 K and at (c),(d) 515 K. Blue circles: measured intensities, black line: Rietveld fit, green line: $I_{\mathrm{obs}} - I_{\mathrm{cal}}$, red line: measured intensities in the paramagnetic phase at 720 K, gray and magenta bars: nuclear and magnetic peak positions, respectively.

experimental determination of the magnetic structure of $SmFeO_3$. Here, we present two complementary neutron measurements where we were able to overcome these obstacles and measure the magnetic structure of $SmFeO_3$ directly. First, we have performed powder neutron diffraction measurements at comparably low neutron energies ($\lambda = 1.8857$ Å) with a special sample geometry at the HRPT diffractometer (SINQ). We were able to overcome the highly neutron absorbing properties of Sm by filling the outer volume of a hollow vanadium cylinder with a special mixture of fine $SmFeO_3$ powder that we "diluted" with fine aluminum powder in order to suppress the Sm absorption effects. As can be seen in Fig. 2, we obtained qualitatively good powder neutron diffraction patterns at 300, 515, and 720 K that could be easily refined with two additional phases of Al and V which do not interfere at all with the $SmFeO_3$ magnetic signal and barely interfere with structural contributions. Therefore, a reliable Rietveld refinement of the magnetic structure of $SmFeO_3$ could be performed.

Since we measured only at temperatures above room temperature, we neglected any Sm ordering [8]. As pointed out in great detail in Ref. [4], there are four different irreducible representations $\Gamma_1^+$, $\Gamma_2^+$, $\Gamma_3^+$, and $\Gamma_4^+$ corresponding to the following four spin configurations for the Fe ordering: $A_xG_yC_z$, $G_xA_yF_z$, $F_xC_yG_z$ and $C_xF_yA_z$ which correspond to the magnetic space groups $Pbnm$, $Pb'n'm$, $Pbn'm'$ and $Pb'nm'$, respectively [9]. Our neutron measurements at 300, 515, and 720 K clearly show that there appears $F_xC_yG_z$-type and $G_xA_yF_z$-type antiferromagnetic ordering in $SmFeO_3$ at 300 and 515 K, respectively. The Rietveld fits of the magnetic intensities are shown in Fig. 2 and the corresponding magnetic moments are listed in Table I in the Supplemental Material [6]. Other spin configurations or incommensurate magnetic structures can be excluded for $SmFeO_3$. We have also performed complementary single crystal neutron diffraction measurements. By choosing an optimized small sample geometry and high incident neutron energies we were able to perform single crystal neutron diffraction measurements at the D9 diffractometer (ILL). The temperature dependence of some prominent magnetic intensities are shown in Fig. 3(a)

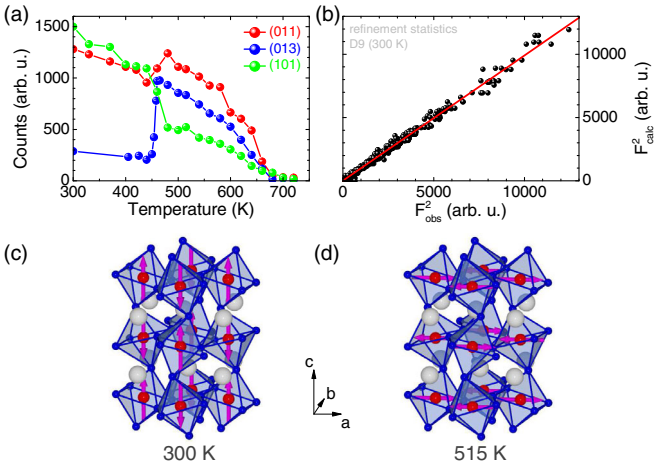


FIG. 3 (color online). (a) Temperature dependence of magnetic intensities measured on our $SmFeO_3$ single crystal at the D9 diffractometer. (b) Refinement statistics of our magnetic and crystal structure refinement of $SmFeO_3$ at 300 K. (c),(d) Magnetic structures of $SmFeO_3$ below and above $T_{SR}$ respectively:

visualizing the spin-reorientation transition. The atomic positions derived from this measurement are very close to the atomic positions derived from a complementary single crystal x-ray diffraction measurement that has been performed on a Bruker D8 VENTURE x-ray diffractometer as well as with values given in literature [10], thus, proving the high reliability of our neutron measurements; see Table I in the Supplemental Material [6]. The comparably good refinement statistics and $R$ values of the structure refinement of this single crystal neutron measurement are shown in Fig. 3(b) and Table I in the Supplemental Material [6]. Finally, we were able to determine the magnetic structure of $SmFeO_3$ and observe a collinear $k = 0$ antiferromagnetic structure; see Figs. 3(c), 3(d). The detection of very tiny canted magnetic moments is beyond the scope of these measurements. As pointed out in Ref. [4] for $SmFeO_3$ (with magnetic ions located at inversion centers), $k = 0$ magnetic structures are not compatible with an inverse Dzyaloshinskii-Moriya interaction induced electric polarization.

The antiferromagnetic properties of $SmFeO_3$ were also studied by linear polarization dependent Fe-$L$ edge x-ray absorption spectra (XAS), conducted at 08B beam line of the National Synchrotron Radiation Research Center (NSRRC) in Taiwan. The spectra were recorded with the total electron yield mode using $Fe_2O_3$ for calibration. X-ray magnetic linear dichroism (XMLD) is the difference in cross section for light polarized perpendicular or parallel to the magnetic moment and is well known to be sensitive to the spin direction of antiferromagnetic systems [11–13]. We have measured the polarization dependent Fe-$L_2$ XAS spectra at 440 and 490 K with the Poynting vector of the light being parallel to the $a$, $b$, and $c$ axis shown in Figs. 4(a)–4(c). We observe a considerable size of the XMLD signals between the electric field $E\|b$ and $E\|c$ in

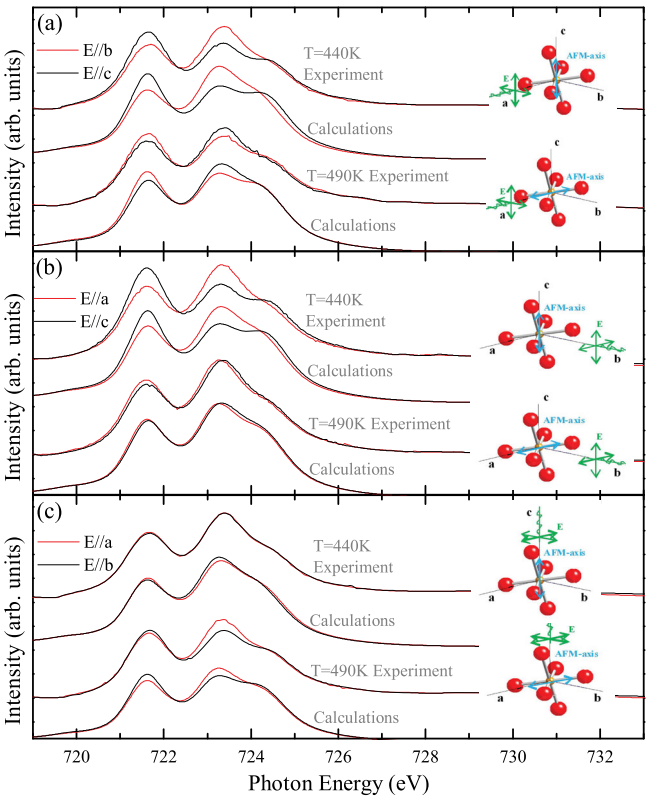


FIG. 4 (color online). Fe $L_{2,3}$ XAS spectra of $SmFeO_3$. (a)–(c) The linear polarization dependent XAS spectra measured above and below $T_{SR}$ with incident beam parallel to $a$, $b$, and $c$ axis.

Fig. 4(a), between $E\|a$ and $E\|c$ in Fig. 4(b), but nearly no difference between $E\|a$ and $E\|b$ in Fig. 4(c). The sign of the XMLD signals is reversed when going from 440 to 490 K; see Figs. 4(a), 4(b). This is similar to the previous study of the Morin transition of hematite [11] revealing a rotation of the spin orientation across $T_{SR}$. To extract the orientations of the antiferromagnetic axes we have simulated the experimental spectra using configuration interaction cluster calculations [14]. The calculated spectra are shown in Figs. 4(a)–4(c) and the parameters used in our calculation are listed in Ref. [15]. The corresponding $FeO_6$ cluster considered in our calculations is also shown in the right part of each figure. One can see that the experimental spectra are nicely reproduced by the calculated spectra with spins parallel to $c$ and $a$ axis at 440 and 490 K, respectively, thus, corroborating the collinear magnetic structure obtained in our neutron measurements.

Also our Fe-$L_{2,3}$ x-ray magnetic circular dichroism (XMCD) spectra as well as our Mössbauer spectroscopy measurements are fully consistent with the fact that there is only one $Fe^{3+}$ species in $SmFeO_3$; see the Supplemental Material [6].

Finally, we measured the anisotropic dielectric properties of single crystalline thin plates of $SmFeO_3$. The capacitance was measured over a range of frequencies with an excitation

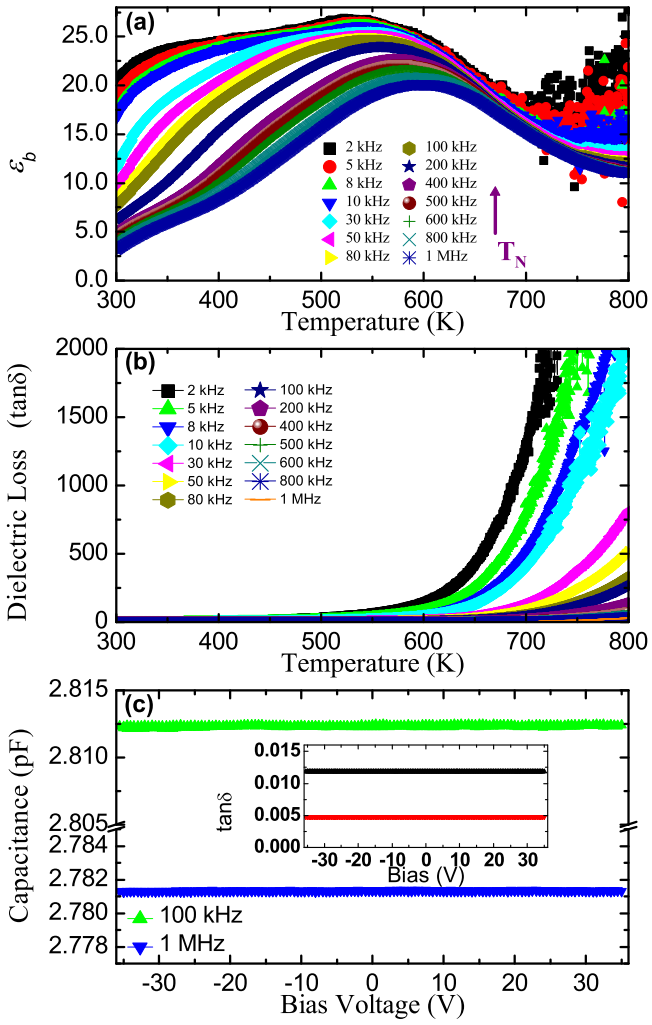


FIG. 5 (color online). Dielectric characterization of $SmFeO_3$ with the electric field along the $b$ axis at different testing frequencies. (a) The temperature-dependent dielectric constant $\varepsilon_b$. (b) The tangent loss $\tan\delta$. (c) The $C$-$V$ curve of $SmFeO_3$ at room temperature with the corresponding loss data in the inset.

level of 1 V, while the temperature was swept at a slow warming or cooling rate (1–2 K/min). As shown in Figs. 5(a), 5(b) the temperature-dependent dielectric constant with electric field along the $b$ axis, $\varepsilon_b(T)$ shows only a broad hump with strong frequency dependence below ~600 K. The dielectric loss, $\tan\delta$, rises strongly as the temperature increases. All samples are insulators at room temperature and become slightly conductive at high temperatures (several kΩ at 800 K). No apparent anomalies could be observed in $\varepsilon_b(T)$ around $T_N$. If an intrinsic ferroelectric transition occurs at $T_N$, the corresponding anomalies should be observable in both $\varepsilon_b$ and $\tan\delta$, irrespective of testing frequencies. Also $\varepsilon_a(T)$ and $\varepsilon_c(T)$ exhibit no anomalies at $T_N$. Complementary capacitance-voltage ($C$-$V$) measurements were carried out for all our samples at room temperature. Fig. 5(c) shows a typical $C$-$V$ curve with the electric field applied along the $b$ axis. No hysteresis could be observed for $SmFeO_3$ within the experimental resolution ($<10^{-4}$).

Hence, we can exclude the existence of ferroelectricity in $SmFeO_3$. We interpret the observations in Ref. [3] differently and suggest that strain could be induced by magnetoeleastic coupling at $T_N$ which then would be responsible for an artificial observation of a pyrocurrent in the $b$ direction at $T_N$. Indeed, our synchrotron radiation powder x-ray diffraction measurements reveal anomalies predominantly of the $b$-lattice parameter of $SmFeO_3$ at $T_N$; see Fig. 1(d). The hysteresis loop reported to occur at 300 K in Ref. [3] may then be attributed to leakage currents [16] which is absent in our experiment. Perhaps this is related to the different lossy character of flux-grown [3] and floating zone grown single crystals.

The absence of ferroelectric properties in $SmFeO_3$ is also consistent with the $k = 0$ magnetic structure that we observed. This has to be contrasted with the case of other isostructural multiferroic materials, like $TbMnO_3$, where non-collinear chiral magnetic structures have been observed [17]. We note that for a $G$-type antiferromagnetic rare-earth orthoferrite $RFeO_3$, the electric polarization induced by exchange striction is known to occur only below the rare earth magnetic ordering temperature which is two orders of magnitude lower than $T_N$ [18]. If exchange striction would be an important mechanism in $SmFeO_3$ one would expect to see also a pyrocurrent signal when the magnetic structure exhibits distinct changes at $T_{SR}$ which is not experimentally observed [3]. Finally, we would like to remark that magnetoelastic effects are not only present in prototypical multiferroic materials like $BiFeO_3$ [19,20] but (across the doping series $Bi_{1-x}La_xFeO_3$ [21]) also in non-ferroelectric centrosymmetric materials like $LaFeO_3$ [22,23]. Our findings suggest that magnetoelastic effects may also lead to an artificial observation of pyrocurrents and, hence, magnetoelastic coupling can easily be misinterpreted as a ferroelectric response.

We thank D. I. Khomskii, M. W. Haverkort, and A. Tsirlin for helpful discussions. We thank H. Borrmann and his team for x-ray diffraction measurements. We thank U. Burkhardt and his team for EDX measurements. This work is partially based on experiments performed at the Swiss spallation neutron source SINQ, Paul Scherrer Institute, Villigen, Switzerland. XMCD experiments were performed at the BL29 Boreas beam line at the ALBA Synchrotron Light Facility with the collaboration of ALBA staff.

*Alexander.Komarek@cpfs.mpg.de

[1] T. Kimura, T. Goto, H. Shintani, K. Ishizaka, T. Arima, and Y. Tokura, Nature (London) **426**, 55 (2003).
[2] S.-W. Cheong and M. Mostovoy, Nat. Mater. **6**, 13 (2007).
[3] J.-H. Lee, Y. K. Jeong, J. H. Park, M.-A. Oak, H. M. Jang, J. Y. Son, and J. F. Scott, Phys. Rev. Lett. **107**, 117201 (2011).

[4] R. D. Johnson, N. Terada, and P. G. Radaelli, Phys. Rev. Lett. **108**, 219701 (2012).
[5] J.-H. Lee, Y. K. Jeong, J. H. Park, M.-A. Oak, H. M. Jang, J. Y. Son, and J. F. Scott, Phys. Rev. Lett. **108**, 219702 (2012).
[6] See Supplemental Material at http://link.aps.org/supplemental/10.1103/PhysRevLett.113.217203, which includes Refs. [3,7,10], for magnetization, Mössbauer and XMCD measurements as well as data of crystal and magnetic structure refinements.
[7] M. Eibschutz, S. Shtrikman, and D. Treves, Phys. Rev. **156**, 562 (1967).
[8] Y. K. Jeong, J.-H. Lee, S.-J. Ahn, and H. M. Jang, Solid State Commun. **152**, 1112 (2012).
[9] E. F. Bertaut, Acta Crystallogr. Sect. A **24**, 217 (1968).
[10] E. N. Maslen, V. A. Streltsov, and N. Ishizawa, Acta Crystallogr. Sect. B **52**, 406 (1996).
[11] P. Kuiper, B. G. Searle, P. Rudolf, L. H. Tjeng, and C. T. Chen, Phys. Rev. Lett. **70**, 1549 (1993).
[12] J. X. Zhang *et al.*, Phys. Rev. Lett. **107**, 147602 (2011).
[13] J. C. Yang *et al.*, Phys. Rev. Lett. **109**, 247606 (2012).
[14] A. Tanaka and T. Jo, J. Phys. Soc. Jpn. **63**, 2788 (1994).
[15] $FeO_6$ cluster parameters [eV]: $U_{dd}=5.0$, $U_{pd}=6.0$, $\Delta=3.0$, $10Dq=1.2$, $\Delta e_g=0.04$, $\Delta t_{2g}=0.02$, $Du=-0.015$, $E_g$Mix $=0.02$, $pd\sigma=-1.4$, and $pd\pi=0.64$, Slater integrals 75% of Hartree-Fock values.
[16] J. F. Scott, J. Phys. Condens. Matter **20**, 021001 (2008).
[17] R. Kajimoto, H. Yoshizawa, H. Shintani, T. Kimura, and Y. Tokura, Phys. Rev. B **70**, 012401 (2004).
[18] Y. Tokunaga, N. Furukawa, H. Sakai, Y. Taguchi, T.-h. Arima, and Y. Tokura, Nat. Mater. **8**, 558 (2009).
[19] S. Lee *et al.*, Phys. Rev. B **88**, 060103 (2013).
[20] J. Park *et al.*, J. Phys. Soc. Jpn. **80**, 114714 (2011).
[21] C. M. Kavanagh, R. J. Goff, A. Daoud-Aladine, P. Lightfoot, and F. D. Morrison, Chem. Mater. **24**, 4563 (2012).
[22] G. L. Beausoleil, P. Price, D. Thomsen, A. Punnoose, R. Ubic, S. Misture, and D. P. Butt, J. Am. Ceram. Soc. **97**, 228 (2014).
[23] S. M. Selbach, J. R. Tolchard, A. Fossdal, and T. Grande, J. Solid State Chem. **196**, 249 (2012).